

Machine-aided Rapid Visual Evaluation of Non-structural Components of Building Façade

Jongseong Choi¹, Chul Min Yeum², Shirley J. Dyke^{1,2}, Mohammad R. Jahanshahi², Francisco Pena², and Gun Wook Park¹

¹ School of Mechanical Engineering, Purdue University, USA

² Lyles School of Civil Engineering, Purdue University, USA





Motivation

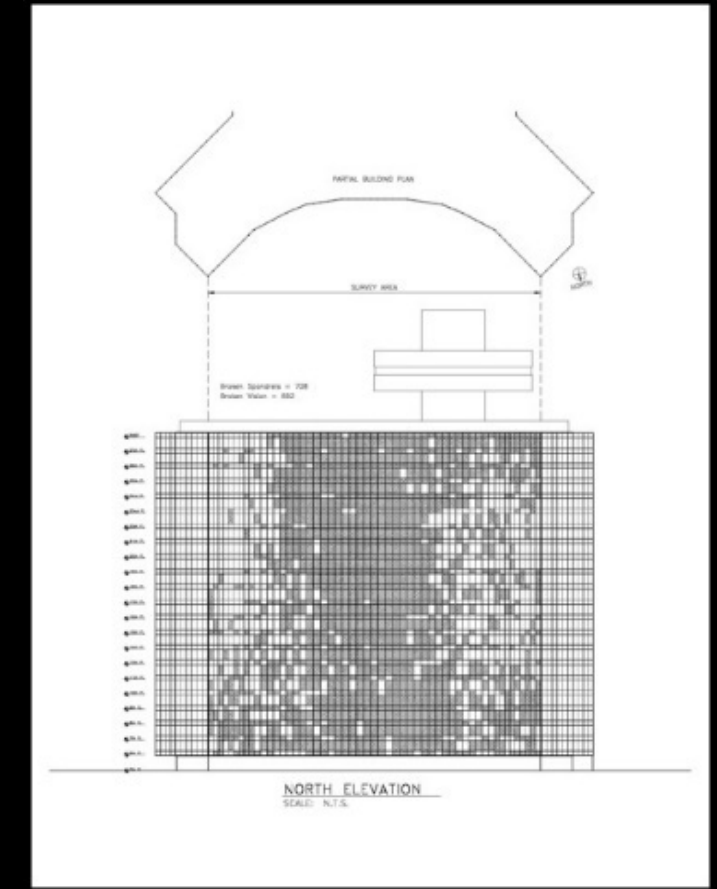
2



**Façade damage
in high-rise buildings**

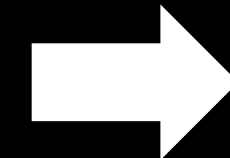
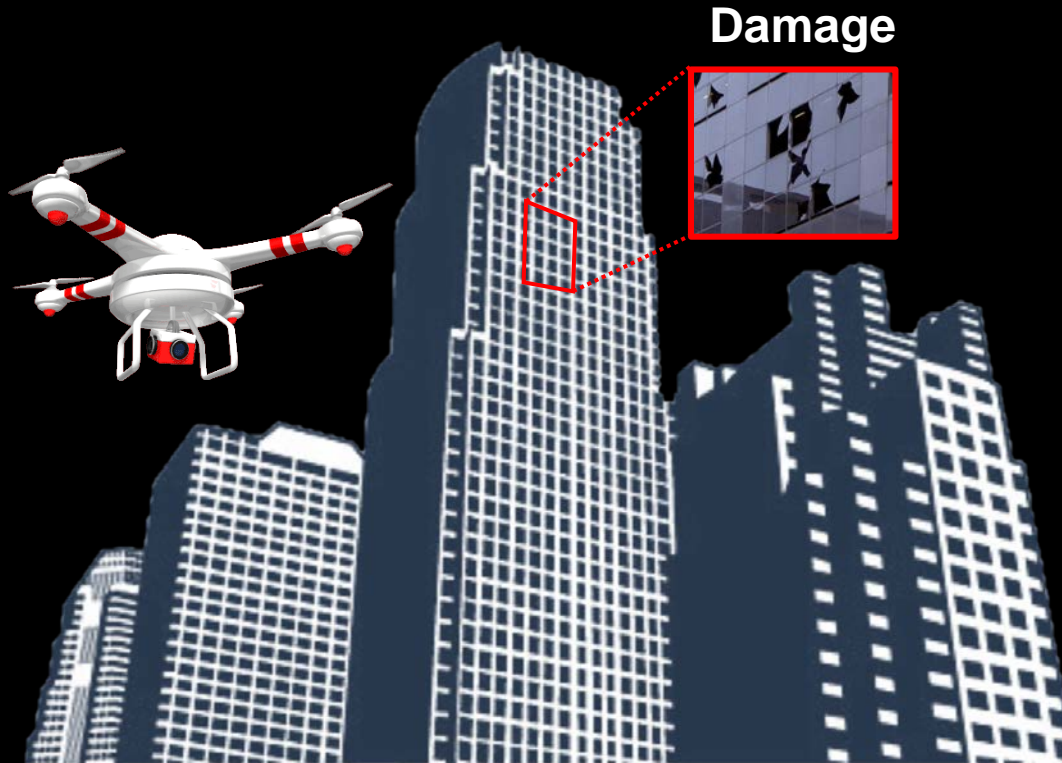


**Restriction of road
& falling hazard**



**Human inspector's
manual annotation**

Opportunity



**Automated visual inspection using
drones**

**A large volume of images collected
from drones**

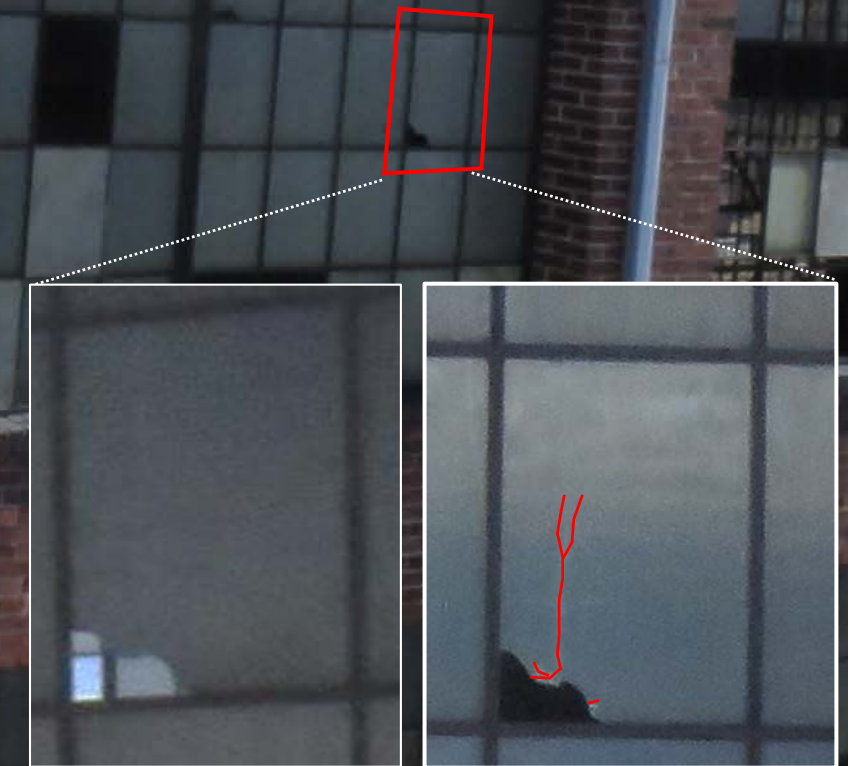
Challenge 1



Challenge 2

TRI:

Target region for Inspection



ROI: Region-of-Interest
Existence of cracks

Challenge 3

TRI:
Target region for Inspection

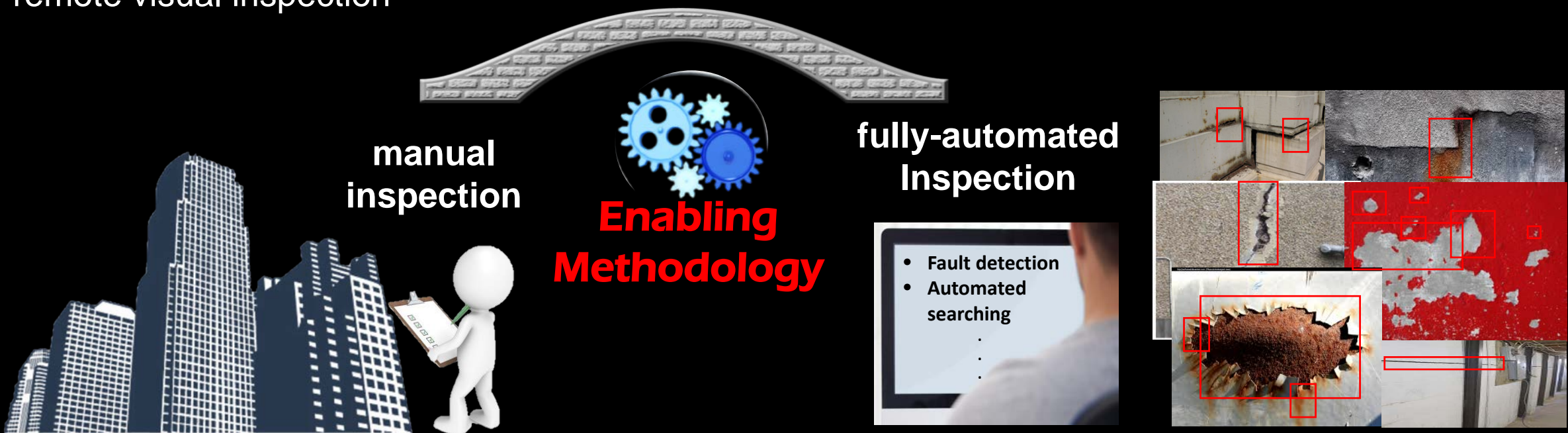


Objective

Develop a **user-friendly application** to support rapid visual inspection of a building façade using images collected by UAVs by automatically constructing **orthophotos** of building façade and extracting **Regions-of-Interest (ROIs)** on each of the collected images so as to process and analyze only highly relevant and localized image areas for visual inspection or damage detection.

Advantage

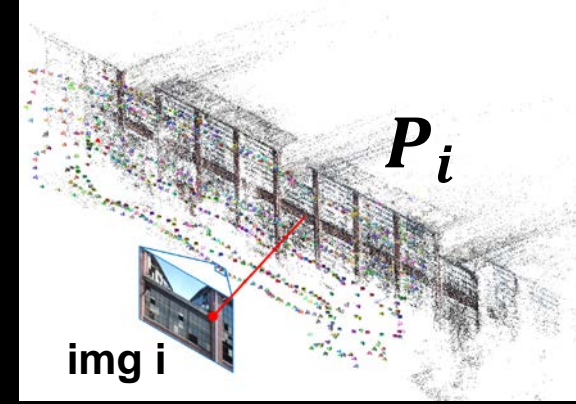
The technique facilitates both human-based visual inspection and applications of existing damage detection techniques on large volumes of actual images in an efficient and reliable way.
; remote visual inspection



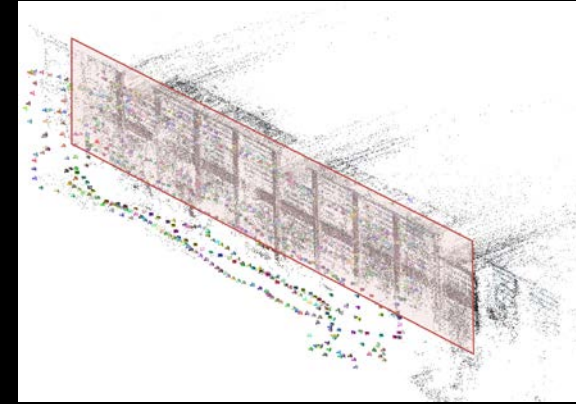
Overview of the Technical Steps



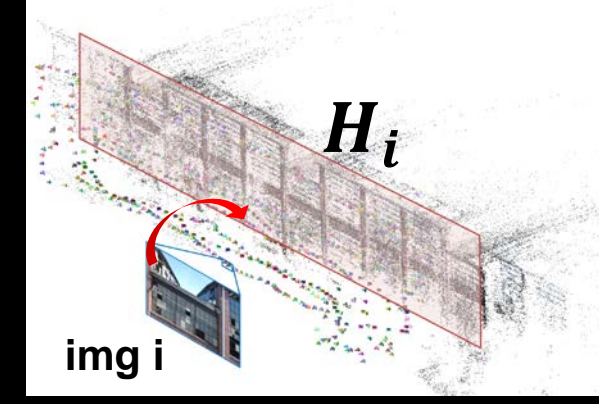
**Step 1: Image collection
using UAVs**



**Step 2: Projection matrix
estimation**



**Step 3: Façade plane
estimation**



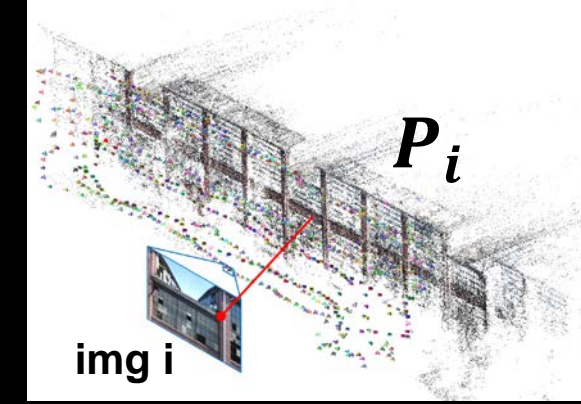
**Step 4: Planar
homography estimation**

Overview of the Technical Steps

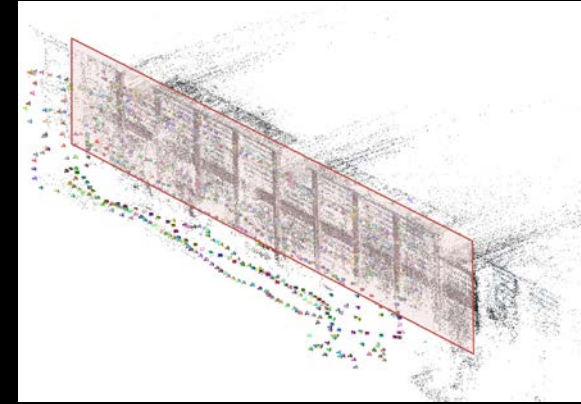


img 1 img 2 ... img n

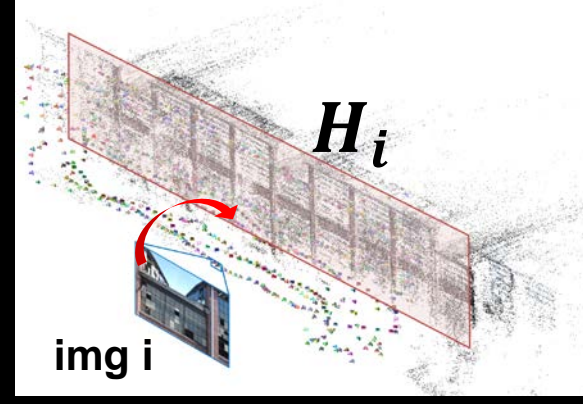
Step 1: Image collection using UAVs



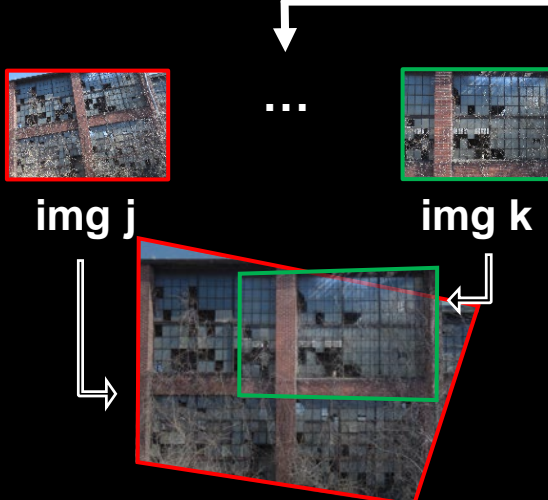
Step 2: Projection matrix estimation



Step 3: Façade plane estimation



Step 4: Planar homography estimation



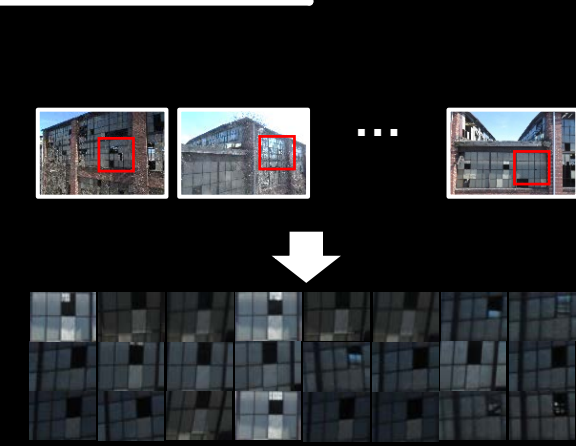
Step 5: Image projection and composition



Step 6: Image blending



Step 7: Selection of a target region of inspection



Step 8: Region of interest localization



Orthophoto Construction

10



A large volume collected images from drone

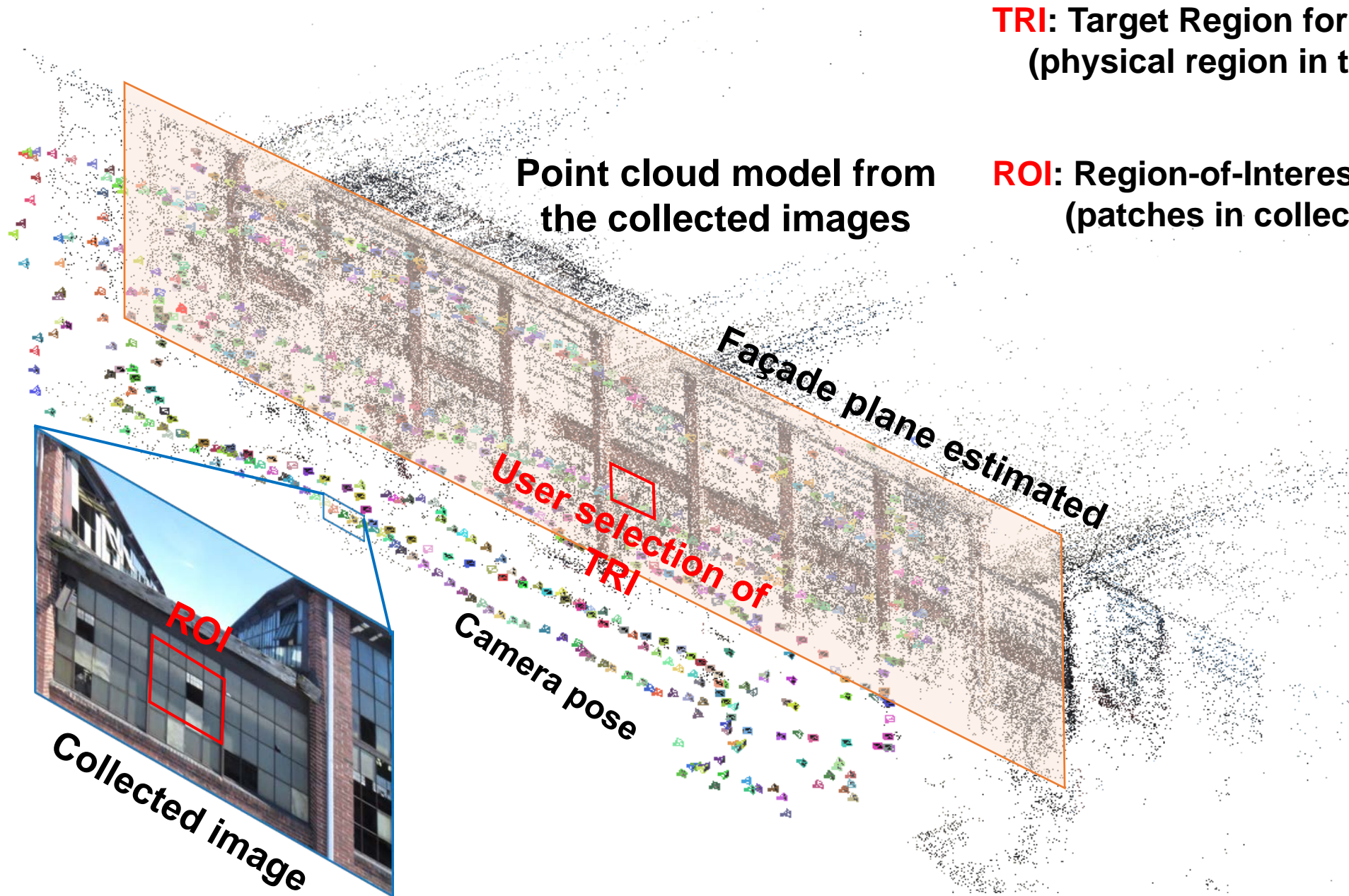


Orthophoto($10,000 \times 3,656$) geometrically connected to each collected images



Mechanism of the tool and ROI extraction

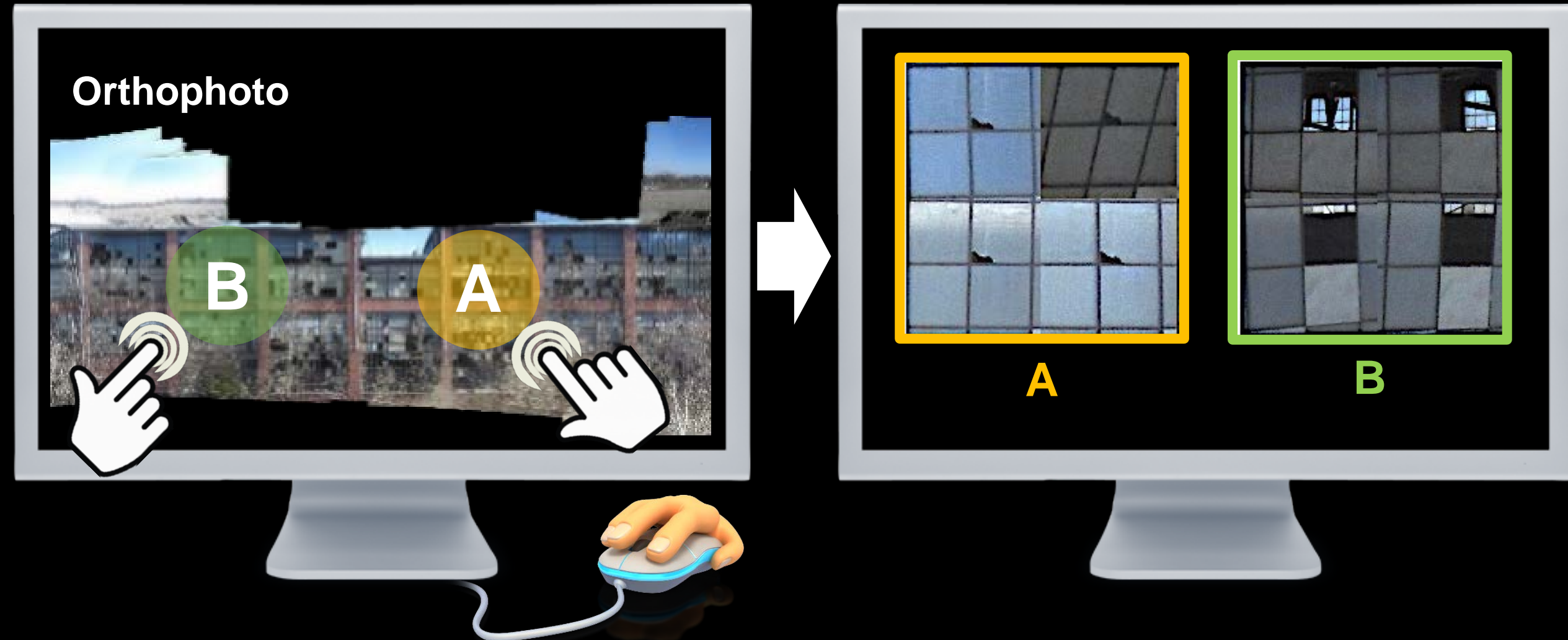
10





User-friendly Applications: Rapid Visual Inspection

11





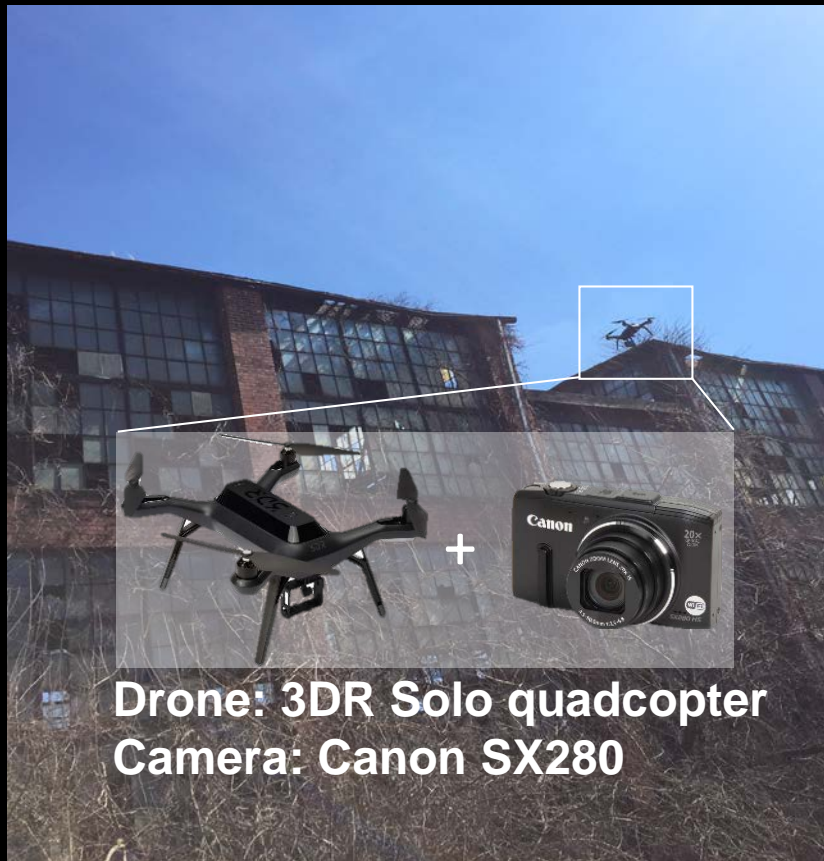
Test Building for Experimental Validation

12

- Consists of window panes, bricks, and external pipes
- Existing damage: cracks and dislocations for windows: bent pipe
- Façade in a post-event situation.



Image Collection Using UAVs



Drone: 3DR Solo quadcopter
Camera: Canon SX280



A total of **1,520** images are collected from the test building with **eight** different flights after viewpoint in the morning and afternoon.

Orthophoto Constructed

15

TRI: Target region for inspection
(physical region in the structure)



TRI 1: Cracked window pane

TRI 2: Cracked pipe



ROI Localization



TRI 1: Cracked window pane

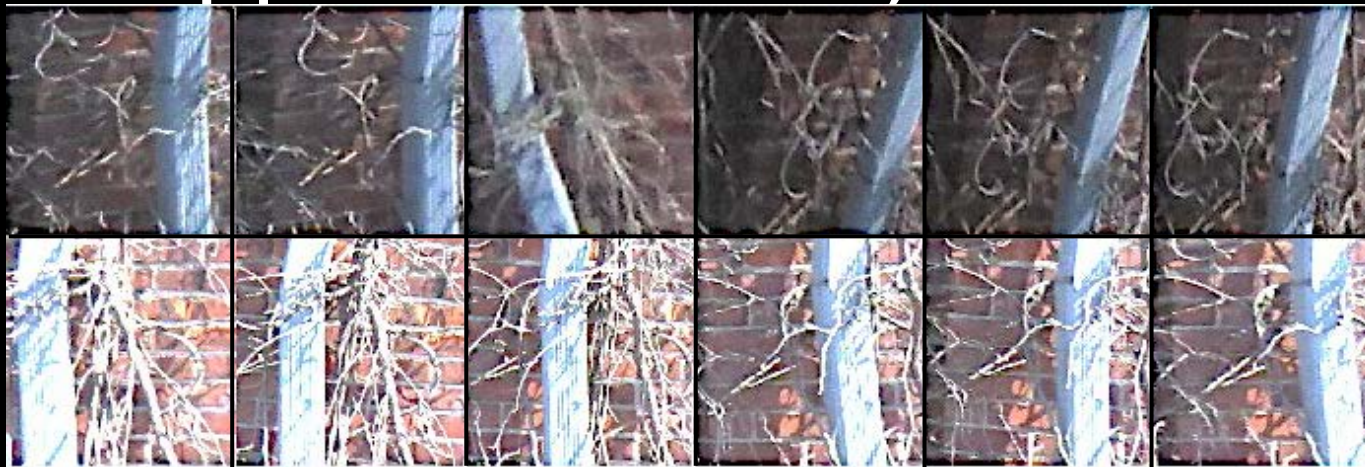
TRI 2: Cracked pipe

Results: Samples of Localized ROIs from TRI 1 & 2

Cracked window pane (74 ROIs extracted)

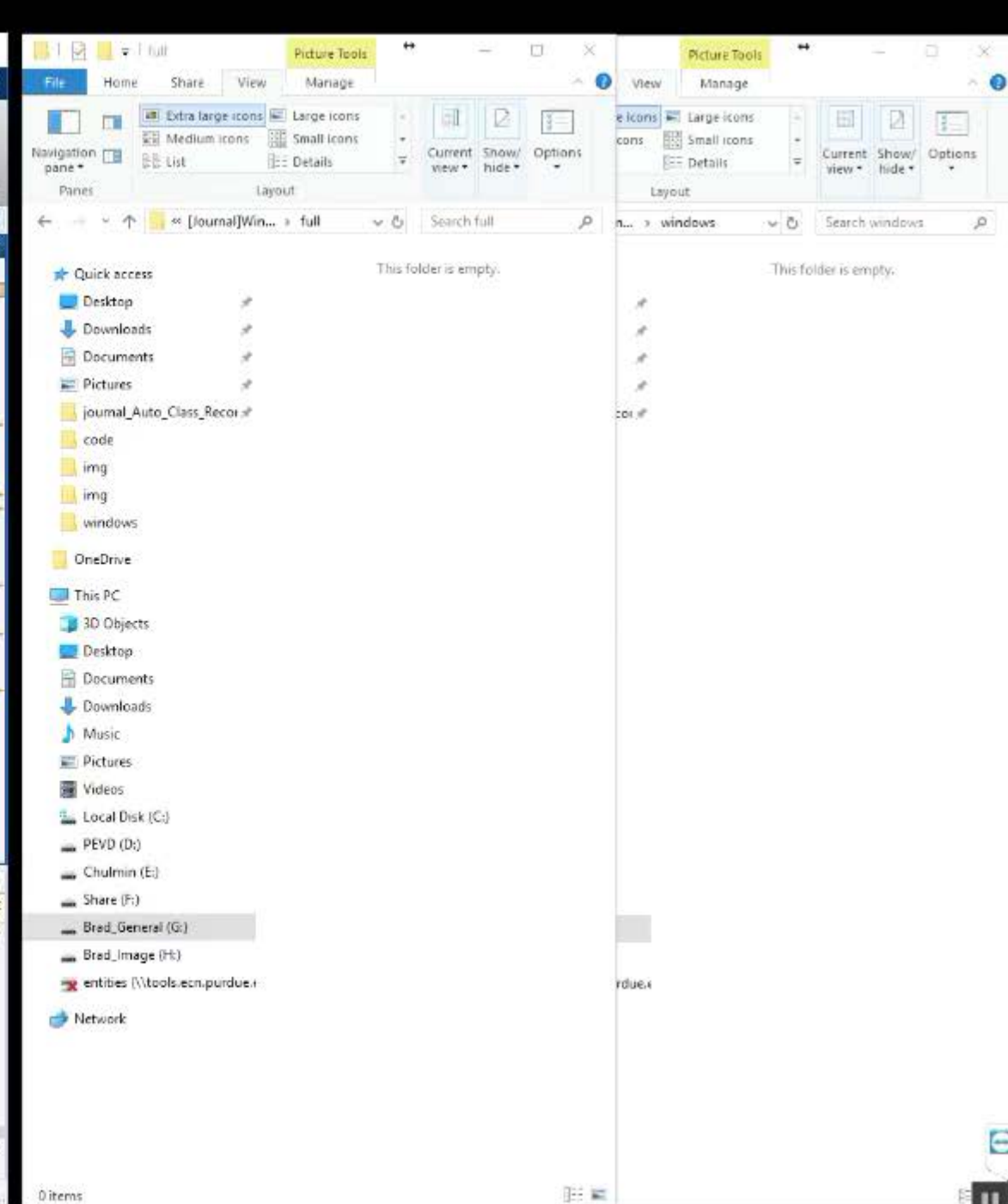
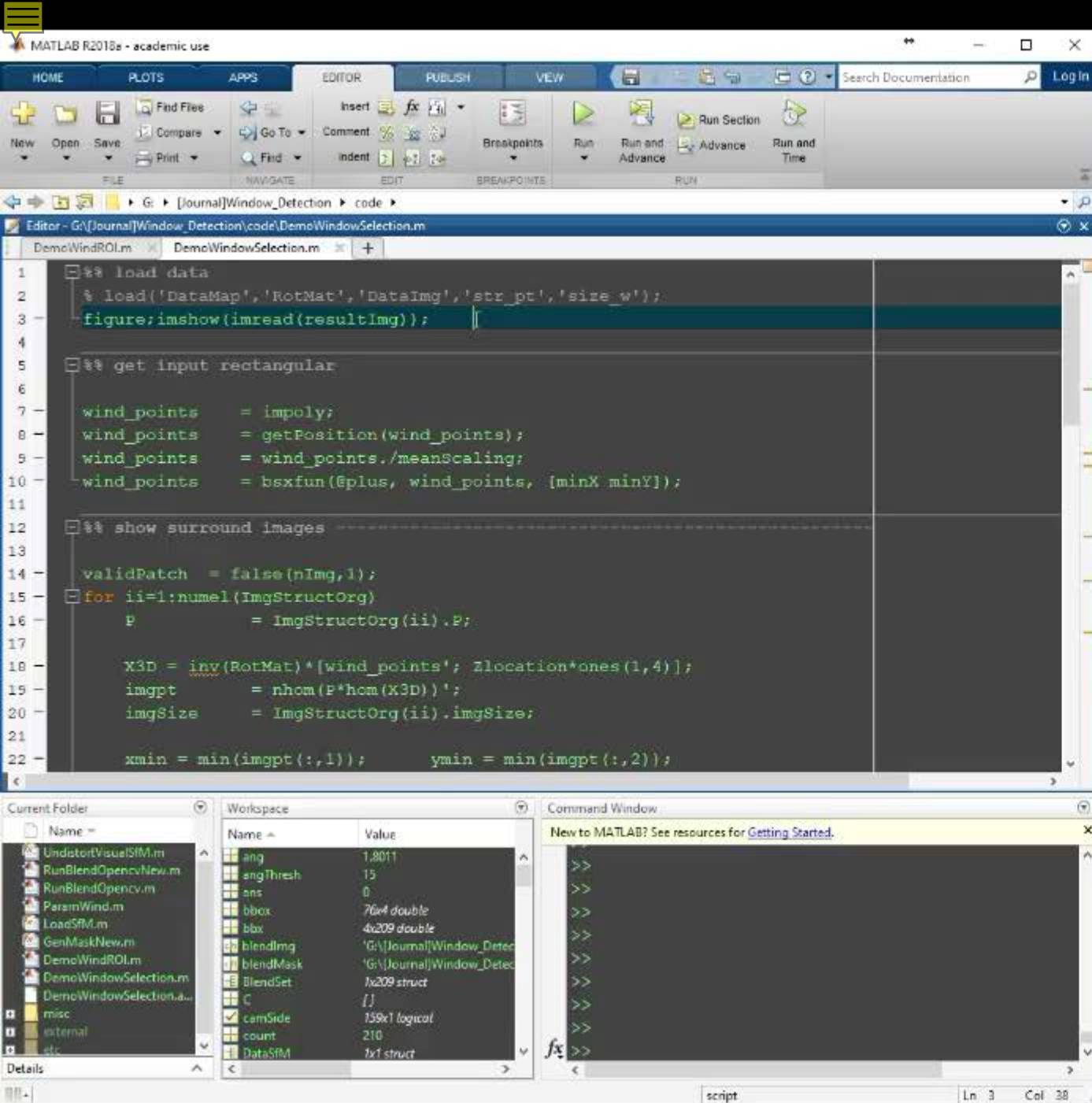


Cracked pipe 53 ROIs extracted)



Demo

**User-friendly Application for
Rapid Visual Assessment**



Processing Time

- **Machine:** A PC workstation having a Xeon E5-2620 CPU and NVidia Tesla k40c with a 12 GB video memory GPU
- **Image Collection:** four-times drone flight: 53 minute
- **SfM processing:** using open-source software, VisualSfM: 3 hours
- **Orthophoto generation:** running in MATLAB: 10 minute
- **ROI localization:** instantly extracted



Related Work

21

Jongseong Choi, Chul Min Yeum, and Shirley J. Dyke, "Active Citizen Engagement to Enable Lifecycle Management of Infrastructure Systems," in preparation (2018).

Chul Min Yeum, Jongseong Choi, and Shirley J. Dyke, "Automated Region-of-Interest Localization and Classification for Vision-based Damage Detection on Civil Infrastructure," Structural Health Monitoring (2017).

Chul Min Yeum, Jongseong Choi, and Shirley J. Dyke, "Autonomous Image Localization for Visual Inspection of Civil Infrastructure." Smart Materials and Structures 26, no. 3 (2017).

Acknowledgement

This work is inspired by a project funded by Indiana Dept. of Trans under project No. SPR-4006.
"Automated (image-based) collection and measurements for construction pay items"

My next presentation will be

EAGER: Active citizen engagement to enable lifecycle management of infrastructure systems (NSF-1645047)





Backup Slides

$$x_i = \mathbf{P}_i X \quad (1)$$

$$\pi X_\pi = 0 \quad (2)$$

$$X_\pi = \mathbf{R} X_\pi \quad (3)$$

where $X_\pi = [a_\pi \ b_\pi \ c_\pi \ 1]^T$ and $\pi = \pi \mathbf{R}^{-1} = [\pi_1 \ \pi_2 \ \pi_3 \ \pi_4]$.

X_π and π in Eq. (3) also hold the relationship in Eq. (2). It becomes

$$\pi_1 a_\pi + \pi_2 b_\pi + \pi_3 c_\pi + \pi_4 = 0 \quad (4)$$

Any X_π on the plane π has a constant value of c_π and satisfy Eq. (4). Since c_π is not correlated with a_π or b_π , c_π becomes:

$$c_\pi = -\pi_4 / \pi_3 \quad (5)$$

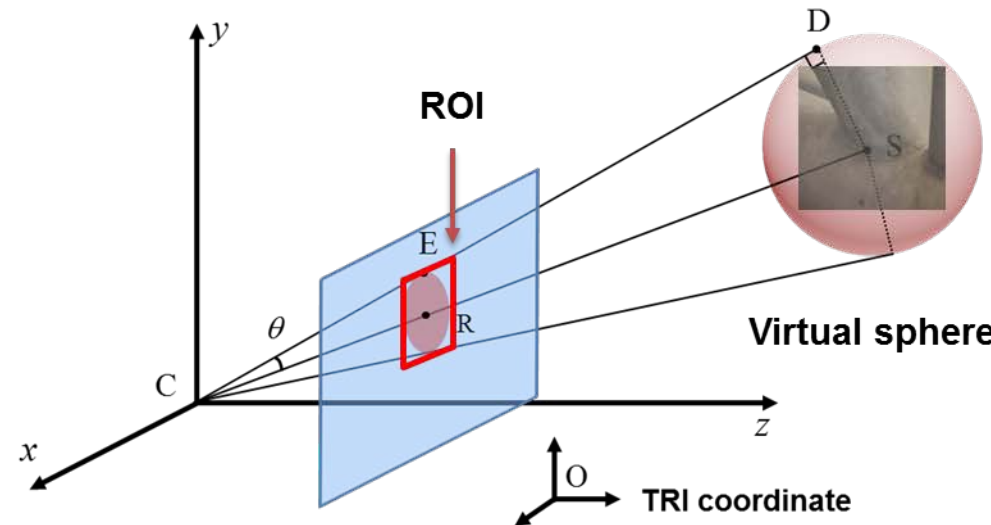
Based on the relations in Eqs. (3) and (4), the homography matrix between π and image i can be computed as:

$$\mathbf{x}_i = \mathbf{H}_{i\pi} \times [a_\pi \ b_\pi \ 1]^T \quad (6)$$

where $\mathbf{H}_{i\pi} = [\mathbf{p}_i^1 \ \mathbf{p}_i^2 \ c_\pi \mathbf{p}_i^3 + \mathbf{p}_i^4]$ and $\mathbf{P}_i = \mathbf{P}_i \mathbf{R}^{-1} = [\mathbf{p}_i^1 \ \mathbf{p}_i^2 \ \mathbf{p}_i^3 \ \mathbf{p}_i^4]$

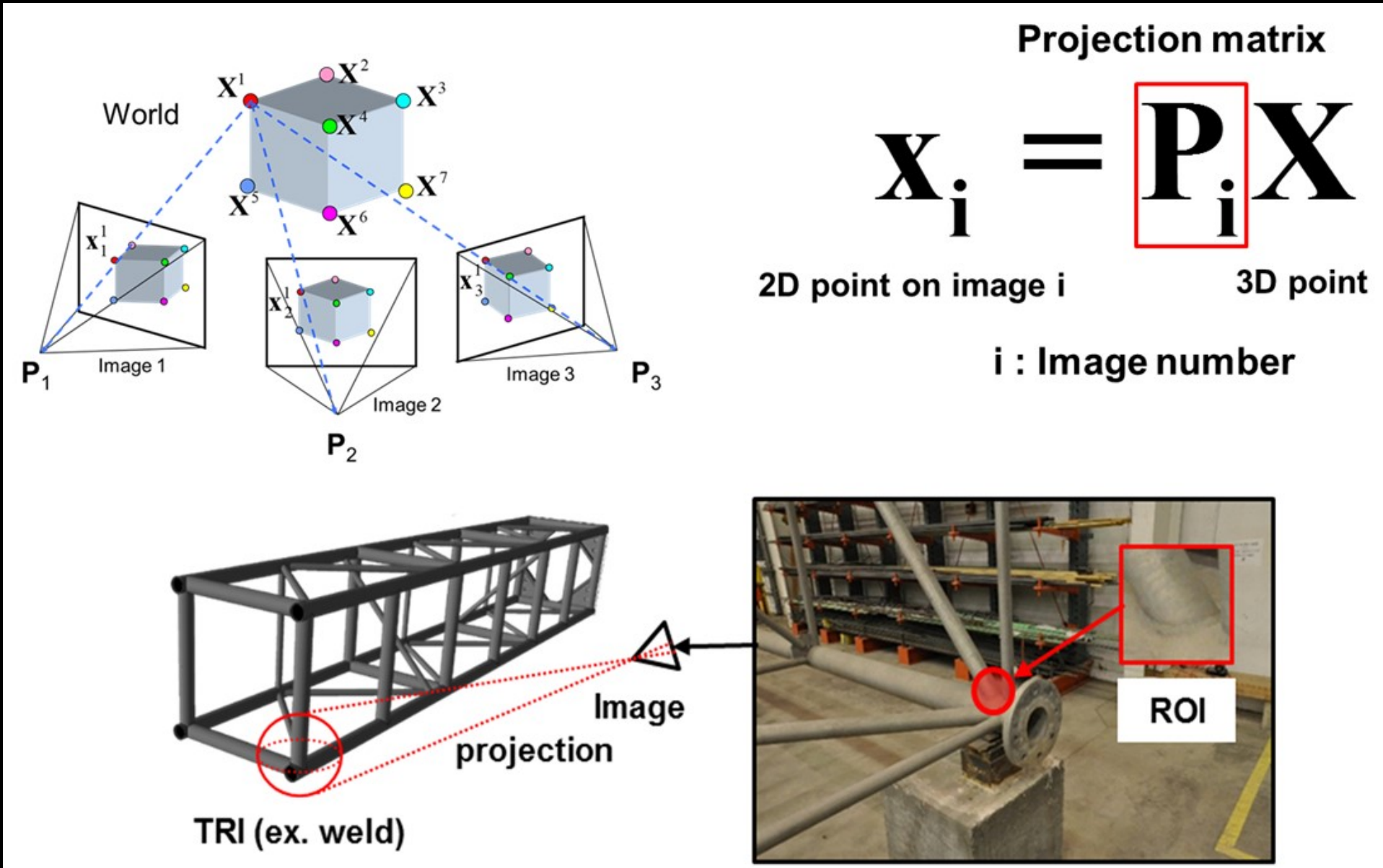
Constraints 1: Bounding boxes
should be entirely visible on the image

Constraints 2: Bounding boxes
should be large enough to obtain
useful ROIs



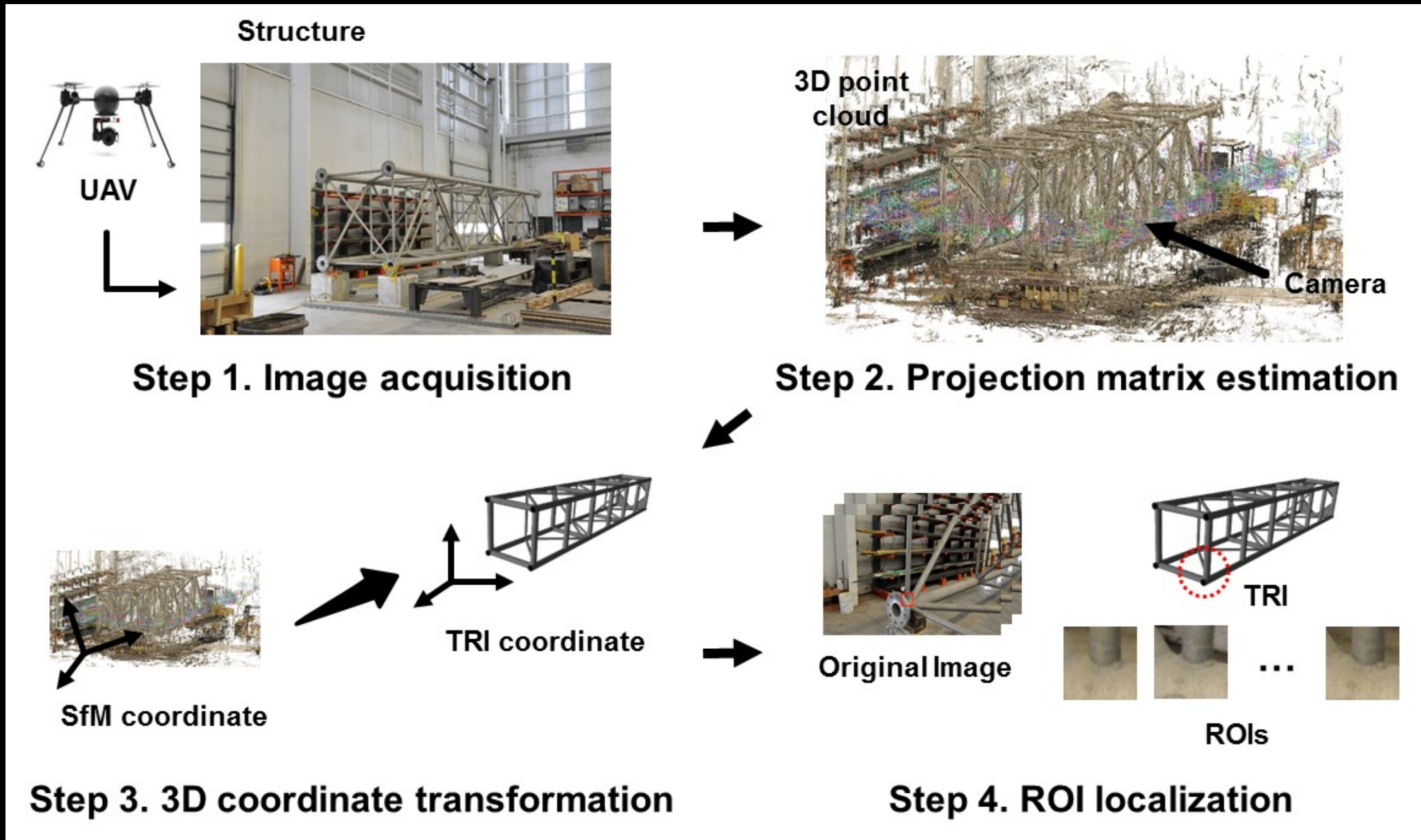


In this study, ROI classification successfully attains a relatively high accuracy. We obtain rates of 89.73% (743/828 images) true-positive (true classification of non-occluded ROIs) and 91.83% (225/245 images) true-negative, respectively. The precision is 97.37%, defined as the number of true-positives over the total number of positives.

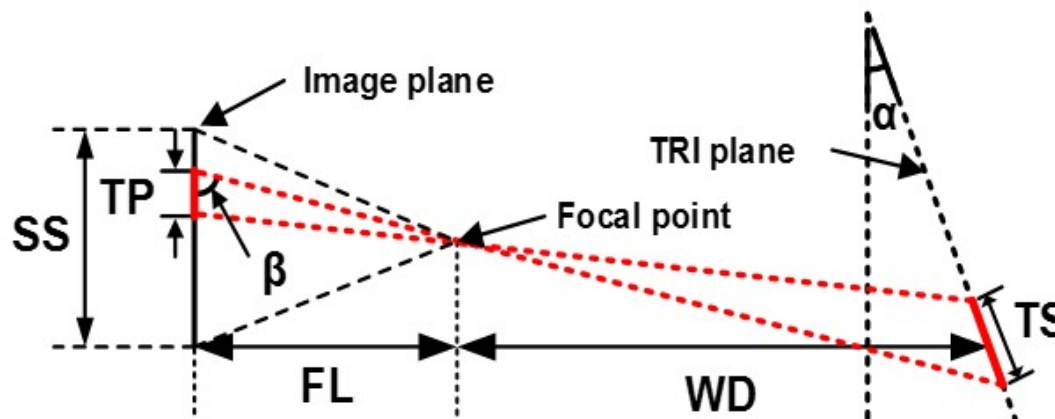


Backup Slide 3

29



1. Working distance



Example

- SR = 4,288 px (Sensor resolution-Width)
- SS = 23.6 mm (Sensor size)
- TS = 63.5 x 2 mm (TRI size – diameter)
- TP = 127 px (the min. size of the ROIs)
- FL = 18 mm (focal length)
- $\alpha = 0 \sim \pi/3$
- $\beta = 0.92 \sim \pi/2$

$$\text{WD} = 2,200 \text{ mm}$$

2. Motion blur

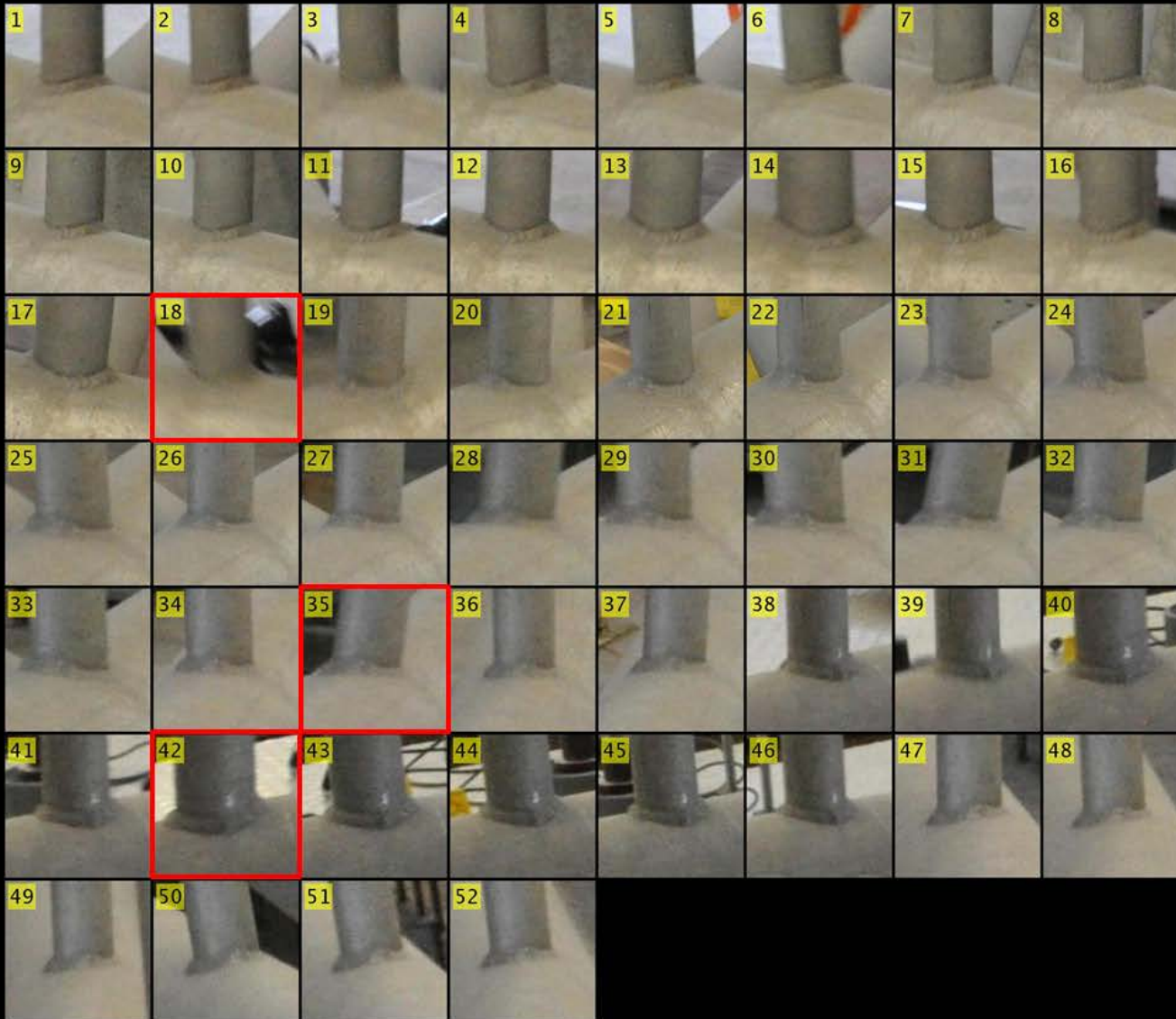
- Flying speed
- Light condition
- Shutter speed
- Vibration on the platform

3. Occlusion



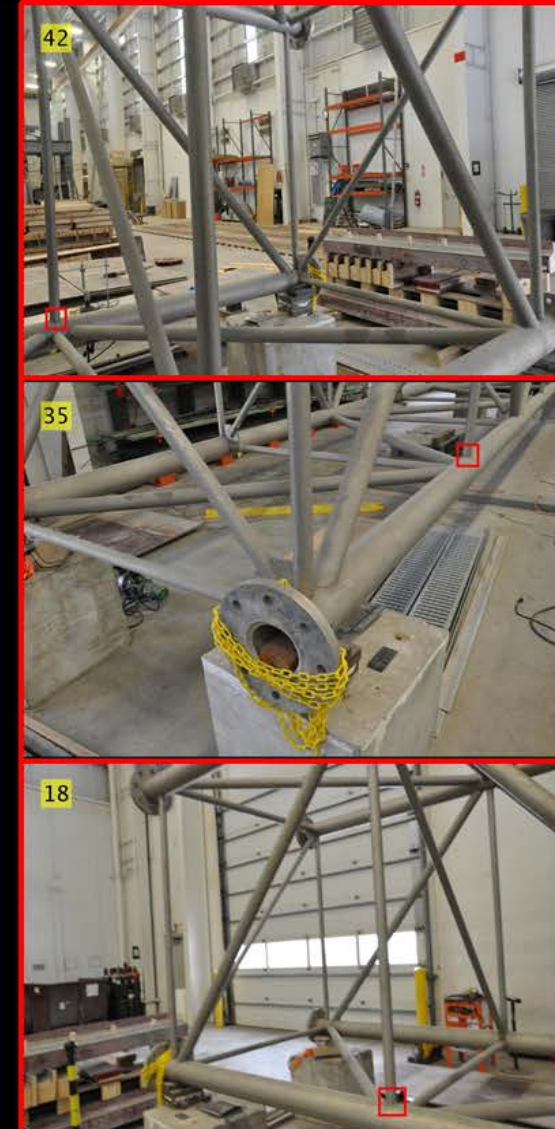
Backup Slide 5

31



ID: Weld_34

Detected images: 52

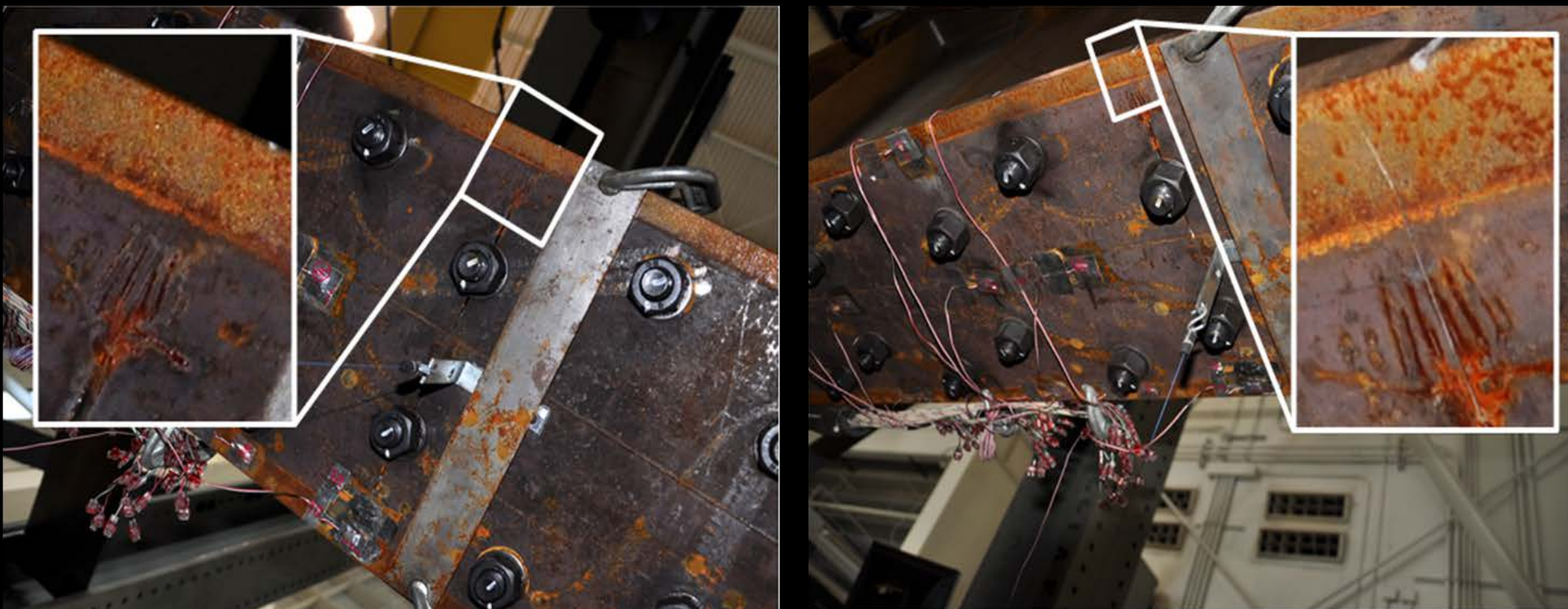


Backup Slide 6

32

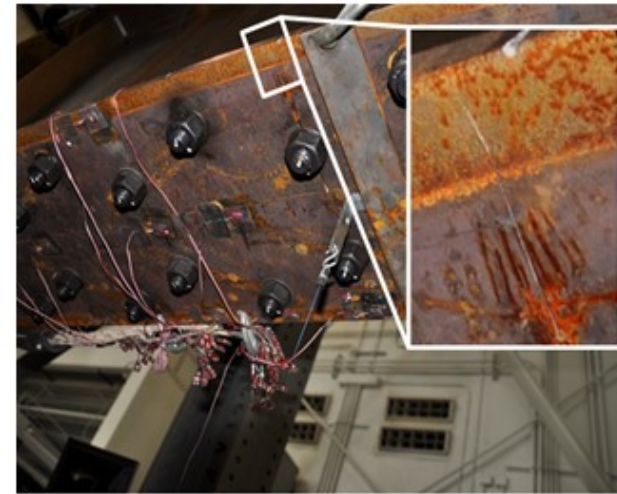


Fatigue testing on a steel girder (courtesy of Matthew H. Hebdon)





Non-crack area



Images of a fatigue crack from different viewpoints

- **Many false-positive alarms and misdetections**
→ **Detection of damage-sensitive areas**
- **Visibility depending on viewpoints**
→ **Use of many different viewpoints of object images**

Backup Slide 6



We train a single binary classifier that is then applied to all welded connections. This approach is possible because the visual appearances of the welded connections are quite similar to each other, and considerably different than the occluded ones in Fig. 6(b). However, if the appearance of the TRIs were visually dissimilar, and common visual features were not shared with each other, multiple classifiers would need to be trained individually for each type of TRI.